Transaction A: Civil Engineering
Vol. 17, No. 4, pp. 273–284

SCIENTIA IRANICA

A New Approach for Estimating the Seismic Soil Pressure on Retaining Walls

S. Maleki[1,*] and S. Mahjoubi[1]

Abstract. *In this paper, a simple finite element model for seismic analysis of retaining walls is introduced. The model incorporates nonlinearity in the behavior of near wall soil, wall flexibility and elastic free field soil response. This model can be employed in nonlinear modeling of retaining walls and bridge abutments. The advantages of this model are simplicity and flexibility in addition to acceptable precision. Using this finite element model, an analytical study is conducted on several soil-wall systems using nonlinear time-history analysis by applying real earthquake records. Based on the results of these analyses, new seismic soil pressure distributions are proposed for different soil and boundary conditions. These distributions are shown to be more accurate than the popular Mononobe-Okabe equations.*

Keywords: *Seismic analysis; Retaining walls; Soil pressure; Soil-structure interaction; Mononobe-Okabe; Finite element analysis.*

INTRODUCTION

Seismic behavior of retaining walls has been widely investigated by researchers since the 1920's. Three pioneer researchers in this field have been Mononobe, Matsuo and Okabe [1,2]. They proposed a pseudo static method to calculate the seismically induced active and passive earth pressures using the Coulomb theory in a wedge of soil behind the wall. The method, herein called the M-O method, gives two relationships for seismic active and passive earth pressures with linear distribution along the wall height. Owing to its simplicity, this method has been widely used by practicing engineers. Seed and Whitman [3] modified the M-O method and suggested new relationships for the seismic soil thrust in terms of unit weight of soil and peak ground acceleration. They also suggested 0.6 H as the resultant force point of action where H is the height of the retaining wall. Anderson et al. [4], by a series of centrifuge tests, found that the location of equivalent dynamic soil pressure forces varies, but recommended a value of 0.5 H for its approximate location. Sherif et al. [5] and Wood [6] proposed a value of 0.45 H above the base for the seismic earth thrust point of action.

1. *Department of Civil Engineering, Sharif University of Technology, Tehran, P.O. Box 11155-9313, Tehran, Iran.*
*. *Corresponding author. E-mail: smaleki@sharif.edu*

Received 14 September 2009; received in revised form 3 March 2010; accepted 17 July 2010

Experimental studies since the 1970's have proved that the M-O method and the modified version (Seed and Whitman method) are satisfactory in calculating the total seismic soil thrust [4,5,7,8].

Another prevalent method used by engineers is the subgrade modulus method. In this method, the soil behind the wall is modeled as a series of parallel massless springs. Using this concept, Scott [9] studied the soil-wall interaction. He modeled the free field soil as a vertical shear beam with mass and the interfacing soil as massless linear springs with constant stiffness. Veletsos and Younan [10] improved Scott's method by applying semi-infinite horizontal bars with constant mass per length connected to the wall by massless linear springs. Richards et al. [11], retrospecting Scott and Veletsos and Younan studies, represented a method of dynamic analysis for retaining walls using a 2D model containing a semi-infinite nonlinear layer of cohesionless soil, free at the top and rigidly restrained at the bottom. The retaining wall is connected to the free field soil by means of elastic constant stiffness springs. They studied the model in four modes of displacement: rotation about base, rotation about top, rigid translation and fixed base. Veletsos and Younan [12], using Lagrange's equation, analyzed a linear model and investigated the effects of many variables, such as base fixity and nonuniformity of the soil shear modulus, on the soil thrust. They concluded that for realistic wall flexibilities, the total wall force is

one half or less of that obtained for a fixed base, rigid wall. They also found the elastic method to be of good precision.

Recently, with great progress in computer software and hardware, nonlinear models have been used by several researchers to investigate many aspects of soil-wall interaction and wall behavior during earthquakes [13-15]. Green and Ebling [16] employed an elasto-plastic constitutive model for the soil in conjunction with the Mohr-Coulomb failure criterion. The wall is modeled with elastic beam elements using a cracked second moment of inertia. Interface elements were used to model the wall-soil interface. Cheng [17] proposed relationships for calculating seismic lateral earth pressure coefficients for cohesive soils using the slip line method. He found iterative analysis to be useful for obtaining passive earth pressure but unimportant for active earth pressure. He also found that active earth pressure is much more influenced by the PGA of an earthquake than passive pressure. Psarropoulos et al. [18] used a finite-element model to study the dynamic earth pressures developed on rigid or flexible nonsliding retaining walls modeling the soil as a viscoelastic continuum. Results showed a crude convergence between the M-O and elasticity-based solutions for structurally or rotationally flexible walls.

More recently, Choudhury and Chatterjee [19], as an extension of the Veletsos and Younan study, used a mass-spring-dashpot dynamic model with two degrees of freedom to arrive at the total active earth pressure under earthquake time history loading. They suggested the use of an influence zone of 10 times the wall height for the soil media behind the wall for dynamic models. They also presented non dimensional design charts for rapid calculation of active earth pressures. Choudhury and Subba Rao, in two different studies, obtained an estimate for the seismic passive earth pressure against retaining walls by using logarithmic spiral and composite curve failure surface assumptions and a pseudo static method [20,21]. Effects of cohesion, surcharge, own weight, wall batter angle, ground surface slope, soil friction angle and seismic accelerations were considered in the analysis.

Although, nowadays, many commercial computer programs with the ability to perform nonlinear analysis of continua are available, these programs are expensive and time-consuming in nonlinear stepwise analyses. Uncertainty regarding the input for soil parameters is also a drawback. Programs like FLAC [22], SHAKE [23] and SASSI [24] are simpler than the general purpose finite element software, but each has its own limitations.

The objective of this paper is to obtain a simplified seismic soil pressure distribution against retaining walls with different boundary and stiffness conditions, such as rigid walls, flexible walls, bridge abutments and propped bridge abutments. Nonlinear finite element dynamic time history analyses of soil-wall systems are employed for verification. It is shown that the suggested equations more accurately predict the seismic soil pressure behind retaining walls than the well-known M-O relationships, and are simple to use.

SOIL-WALL MODEL

In this section, the theoretical background for construction of an accurate finite element soil-wall analysis model is described. Past research has been selectively put together to obtain a simple but yet accurate model that ignores nonlinearity in the far field soil but captures it in the near field soil adjacent to the wall where it most affects the wall pressure.

In an earthquake, the soil-wall system can experience considerable displacement. If the wall and the free field displacement of the soil are equal, then the wall has no effect on the free field soil stresses. However, this is usually not the case, and the difference in displacements of the soil and wall creates stresses in the soil, especially in the vicinity of the wall. Therefore, the horizontal stresses in the soil behind the wall can be written in terms of the difference between the free field soil and wall displacements. This phenomenon can be modeled with nonlinear springs attached to the wall representing the interfacing soil. In addition, the free field soil can be modeled with elastic plane strain shell elements. These are further explained below.

In general, the wall displacement can be obtained as:

$$u_w = u_f - \Delta u, \tag{1}$$

where u_f is the free field soil displacement, u_w is the wall displacement and Δu is the difference between the wall and free field soil displacements (Figure 1). The total soil stress behind the wall for increment i (at location of spring i) can be written as:

$$\sigma^i_{wn} = \sigma^i_{fn} + \Delta\sigma^i_n, \tag{2}$$

$$\Delta\sigma^i_n = k^i_s(u^i_{fn} - u^i_{wn}). \tag{3}$$

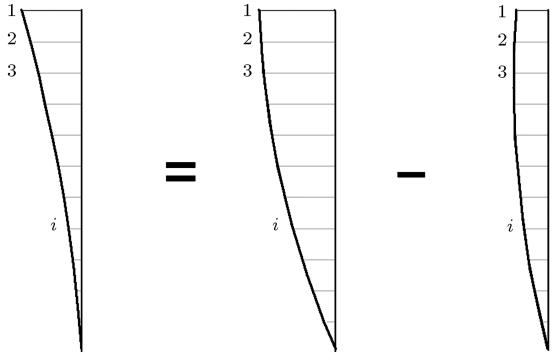

Figure 1. Typical soil and wall displacements.

σ^i_{wn} = total soil normal stress against the wall at increment i (at location of spring i).
σ^i_{fn} = normal soil stress in free field at increment i.
$\Delta\sigma^i_n$ = variation of soil stress because of the difference between the free field soil and wall displacements at increment i.
k^i_s = soil subgrade modulus at increment i.

The total horizontal force behind the wall is:

$$P_{nt} = \int_0^H \sigma_{wn} dz, \tag{4}$$

and the overturning moment is:

$$M_{nt} = \int_0^H \sigma_{wn} z dz. \tag{5}$$

Therefore, the point of application of the resultant horizontal force is obtained as:

$$h_0 = \frac{M_{nt}}{P_{nt}}. \tag{6}$$

For cohesionless soils, the modulus of elasticity (E) and the shear modulus (G) vary increasingly with depth. Two common assumptions for this variation are linear and parabolic. Here, the parabolic assumption is used for the shear modulus as follows [11]:

$$G_z = G_H . \sqrt{z/H}, \tag{7}$$

where G_z and G_H are the elastic shear moduli at depths z and H, respectively.

The soil behind the wall is divided into layers and the above equation is used to estimate G in the middle of each layer. The equivalent springs representing the soil adjacent to the wall are modeled using nonlinear link elements. The stiffness of each spring, defined as the subgrade modulus, is derived as follows [9]:

$$k_s = C_z . \frac{G_z}{H}, \tag{8}$$

where C_z is a constant representing the geometric properties of the model. The value of C_z is assumed to be 1.35 based on the suggestion of Huang [11,25]. Soil pressure is considered bounded by the active and passive soil pressures as follows:

$$K_a . \gamma . z \leq \sigma_z \leq K_p . \gamma . z, \tag{9}$$

where:

$$K_a = \frac{1 - \sin\phi}{1 + \sin\phi}, \qquad K_p = \frac{1 + \sin\phi}{1 - \sin\phi}. \tag{10}$$

Therefore, the springs between the free field soil and retaining wall are modeled as a bilinear elastic perfectly plastic type. The initial elastic linear part stiffness is calculated from Equation 8 by substituting G_z for each spring from Equation 7. The plastic portion has a maximum/minimum force of P_p/P_a. These are spring forces equivalent to passive and active soil pressures, respectively, and are calculated by multiplying passive or active soil pressures and the spring corresponding area for each spring. A typical force-displacement plot for soil springs between the retaining wall and the free field soil is shown in Figure 2.

Figure 3 shows the structural model of the soil-wall system. The wall is modeled by using shell elements of concrete. The width of the wall and soil shell elements, perpendicular to the paper in Figure 3, is considered to be 1 meter.

The free field soil modeling in this study consists of an infinite half-space elastic layer of dense cohesionless soil with unit weight of γ. This half-space layer

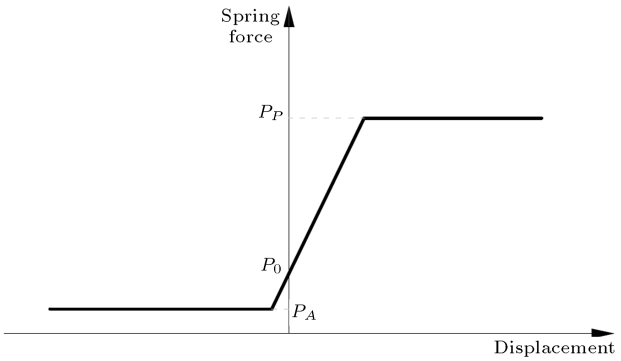

Figure 2. Typical force-displacement plot for soil springs behind a retaining wall.

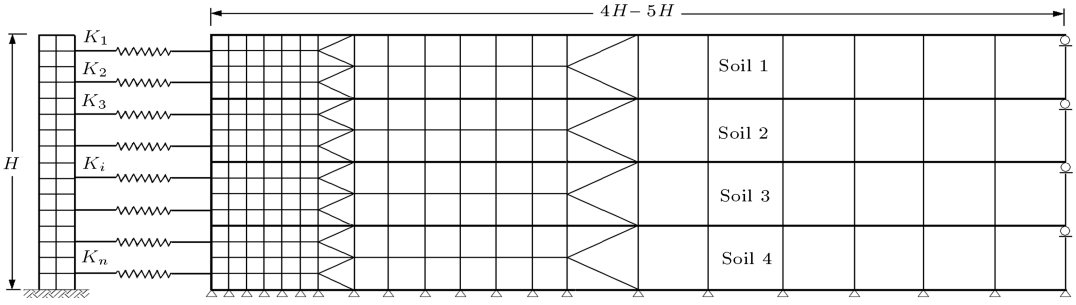

Figure 3. Soil-wall finite element model.

is free at the top and considered fixed at the bottom where similar soil acceleration is applied to the soil and wall during an earthquake. Free field soil is assumed to have a finite length equal to 4 to 5 times its thickness. Choudhury and Chatterjee suggested an influence zone of 10 times the wall height for the soil media behind the wall [19]. However, in their study, soil media at the end is not restrained against vertical displacement, which is the case in this study (Figure 3). The authors found that restraining the end of the soil media against vertical displacement decreases the influence zone and makes the model smaller and more efficient.

The height of the retaining wall and the soil behind it are assumed to be the same and equal to H. The free field soil layer is modeled using plane strain elements. Soil layers have different elastic properties; however, they are assumed to be constant within each soil layer. Shear modulus is calculated by substituting the average depth of the layer as z in Equation 7. Poisson's ratio for all soil layers is assumed to be 0.3.

Four different cases of rigid retaining wall, flexible cantilever retaining wall, bridge abutment and propped bridge abutment are considered, each with 4 m, 6 m and 8 m wall heights. In the case of a rigid retaining wall, it is assumed that the wall has unlimited stiffness and so shows no deformation. Although in reality this is impossible, the case of a buttressed wall comes very close to this assumption.

The flexible wall case is the case of a cantilever retaining wall with variable thickness. It is assumed that the thickness varies from 0.3 m at the top to 0.1 H at the bottom. In the case of a 4 m flexible wall, it is not practical to vary the wall thickness from 0.3 m to 0.4 m. Therefore, the wall thickness is considered to be constant and equal to 0.4 m.

In the case of bridge abutments, the wall thickness is considered to be constant throughout the height. The thickness is assumed to be equal to 1 m for 6 m and 8 m height walls and 0.8 m for a 4 m height wall. The case of a propped bridge abutment is a special case of bridge abutment in which the superstructure restrains the abutment horizontally at the top. Although in reality this restraining is limited, the case is valuable as an extreme boundary condition case.

In all cases considered for analyses, the wall is fully restrained at the bottom (rotations and displacements). However, the effect of foundation rotational stiffness is investigated separately for a 6 m high bridge abutment and the propped bridge abutment models. In these models, the restraint against rotation at the bottom of the wall is removed and a rotational spring is substituted to model the foundation and soil rotational stiffness.

In bridge structures, the superstructure connection to the abutment can be categorized into two main groups: free and restrained. If the superstructure is not restrained to the abutment, the gap between the backwall and the superstructure is usually closed by the superstructure movements and, most of the time, the collision of the superstructure into the backwall is unavoidable in severe earthquakes. This collision produces a considerable concentrated force at the top of the bridge abutment. In the second case where the superstructure is restrained to the abutment, the superstructure inertial force is transferred to the abutment through the restraint as a concentrated force at the abutment seat level. Therefore, abutments have to resist a considerable concentrated force at their top during earthquakes in both cases. However, the effect of a superstructure horizontal force on top of the abutment is usually ignored in bridge abutment design. To evaluate the effect of this force and determine the part of this force taken by the soil behind the abutment, a concentrated force with variable value is considered to push the wall against the soil at the assumed superstructure center of mass, as is the case during earthquakes.

Ground motions of 6 historical earthquakes (the 1940 El Centro, the 1989 Loma Prieta, the 1992 Landers, the 1986 Palm Spring, the 1971 San Fernando (at Pacoima dam station) and the 1966 Parkfield) are used in nonlinear time-history analyses. Figure 4 shows the pseudo acceleration (PSA) spectrum for ground motions used in the analyses.

ANALYSES RESULTS

Nonlinear finite element dynamic time history analyses on the soil-wall systems described above are performed. Soil pressure is calculated from the spring forces output divided by the distance between the springs and the

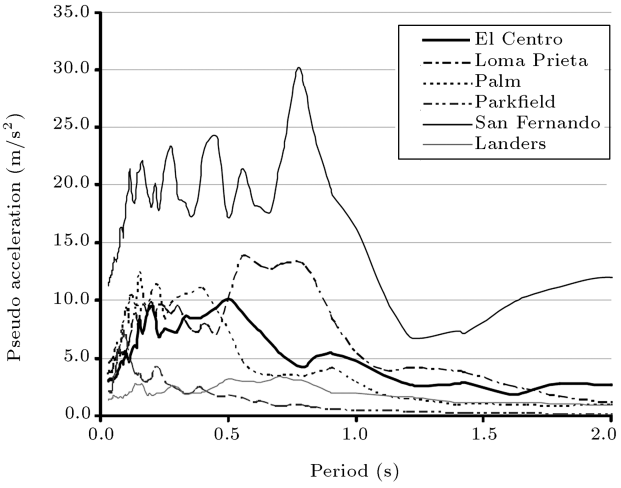

Figure 4. Pseudo acceleration (PSA) spectra for selected ground motions.

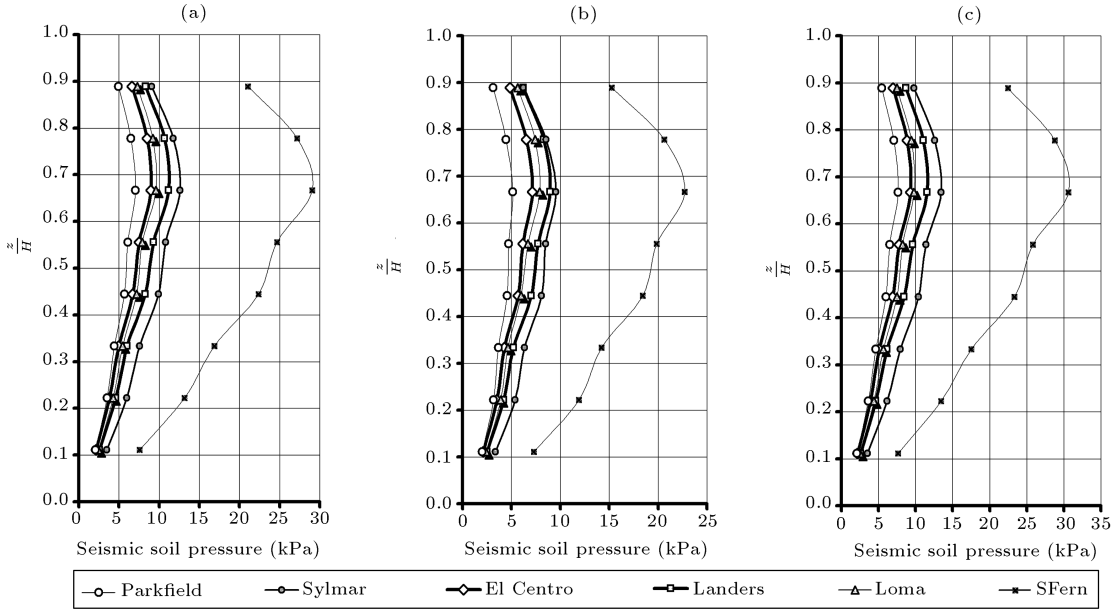

Figure 5. Seismic soil pressure for 4 m height wall. (a) Bridge abutment; (b) flexible wall; (c) rigid wall.

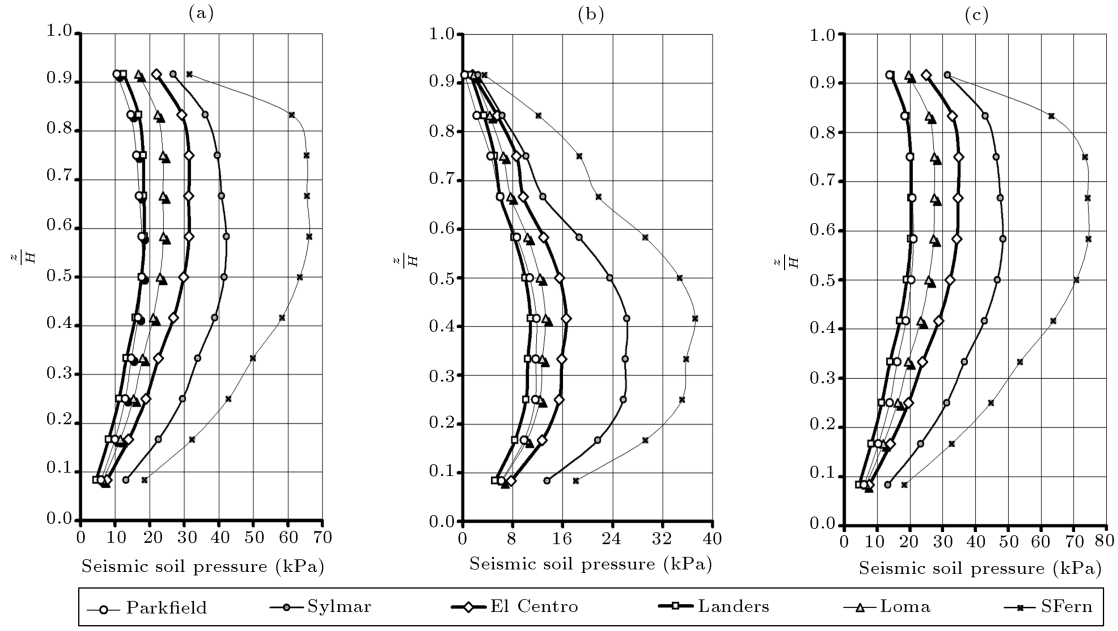

Figure 6. Seismic soil pressure for 6 m height wall. (a) Bridge abutment; (b) flexible wall; (c) rigid wall.

element's thickness (1 m). Plots of soil pressure versus z/H for the 6 ground motions are shown in Figures 5-7.

As can be seen in Figure 5 for the 4 m high wall, the seismic soil pressures for different cases have a similar distribution, but are slightly different in maximum values. However, this is not the case in 6 m and 8 m high walls (Figures 6 and 7). For these walls, the distribution for flexible walls is very different from that of rigid, propped and abutment walls, which have similar distributions. In fact, distribution is dependent on wall flexibility. In other words, for 4 m high walls, all cantilever walls act as rigid walls whereas for 6 m and 8 m high walls, the cantilever retaining walls are more flexible and reduce soil pressure. Bridge abutments and propped bridge abutments with all wall heights considered here (4 m, 6 m and 8 m height) show similar soil pressure distributions as rigid walls, but have less maximum seismic soil pressure. It should be noted that the above seismic soil pressures resulted from analyses must be added to the active or at rest soil pressures to obtain the total soil pressures behind the retaining walls.

To evaluate the effects of foundation rotational stiffness on seismic soil pressure, the restrained base

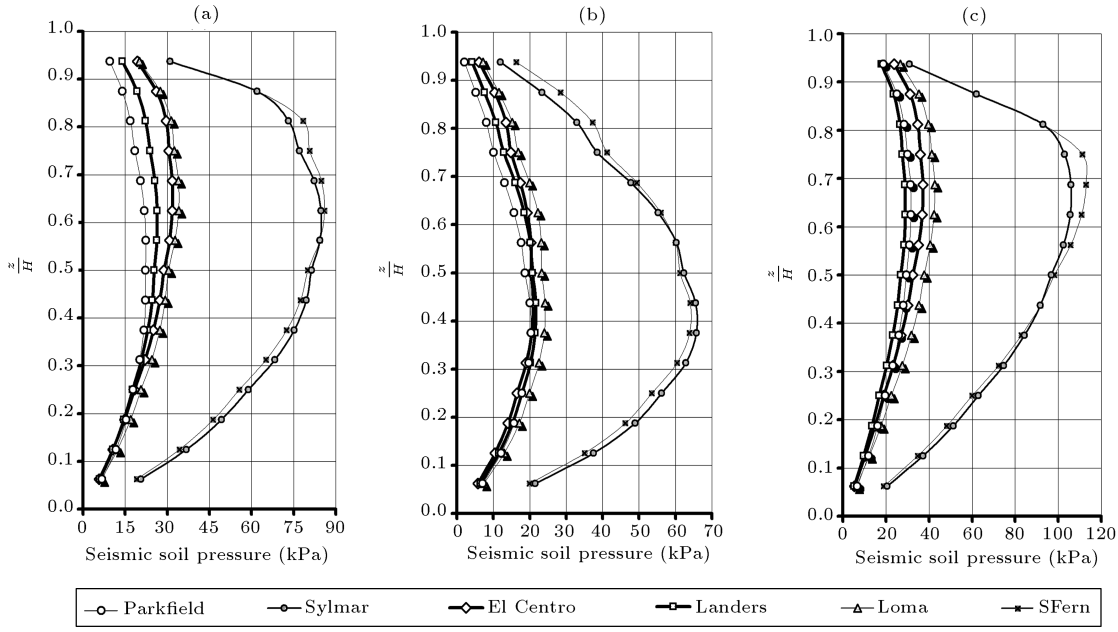

Figure 7. Seismic soil pressure for 8 m height wall. (a) Bridge abutment; (b) flexible wall; (c) rigid wall.

of the 6 m high wall is replaced with a rotational spring of varying stiffness. Results of the nonlinear analyses using the El Centro ground motion are shown in Figure 8. As can be seen in Figure 8, the results show a great dependence on base rotational stiffness. For instance, variation of base rotational stiffness from 10^5 kN.m/rad/m to 10^6 kN.m/rad/m increases the total soil thrust by about 103%.

Figure 9 illustrates the soil pressure distribution due to external concentrated force at the abutment top. This force is applied along the assumed superstructure's center of mass. This pressure also should be added to at rest soil pressure to acquire total soil pressure. As can be observed in Figure 9, the external concentrated force at the top of the abutment increases the soil pressure in the upper part. If the external force value is great enough, it can push the soil into the passive state in that region. By increasing the external force, the depth of this passive earth pressure (passive depth) is also increased. One can conclude from Figure 9 that the external concentrated force affects taller walls more severely. For instance 4.7% of a 1500 kN concentrated force on a 4 m high abutment wall is taken by the soil, whereas this ratio is 29.1% for an 8 m high abutment wall.

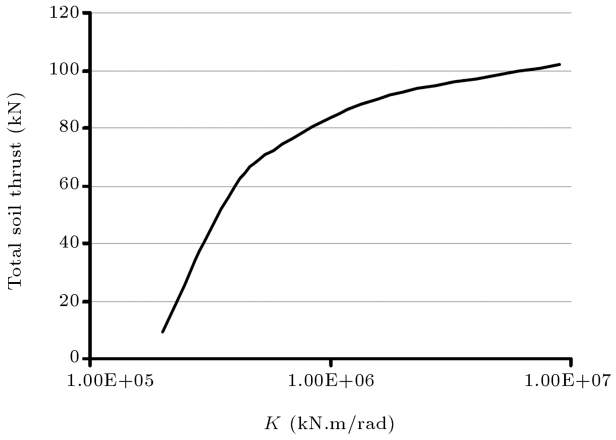

Figure 8. Effect of base rotational stiffness on total seismic soil thrust.

SUGGESTED SEISMIC SOIL PRESSURE DISTRIBUTION

Several seismic soil pressure distributions along the wall height are suggested by researchers [26]. For example the M-O method suggests a linear distribution, but the Seed and Whitman method suggests no distribution and only defines 0.6 H as the seismic thrust point of action.

Based on the results of this study, two approximate distributions of seismic soil pressures are proposed, as shown in Figure 10. Type I distribution is a typical distribution suggested here for rigid walls and semi-rigid walls, such as bridge abutment and propped bridge abutment. Type II distribution is a distribution suggested for flexible walls such as cantilever retaining walls taller than 5 m. It is suggested that the maximum seismic soil pressure, q_0, be obtained from one of the three equations below. Equation 11 uses the Peak Ground Acceleration (PGA) of an earthquake. Equation 12 uses the area under the pseudo acceleration response spectrum (PSA) of an earthquake, whereas Equation 13 uses the peak spectral acceleration.

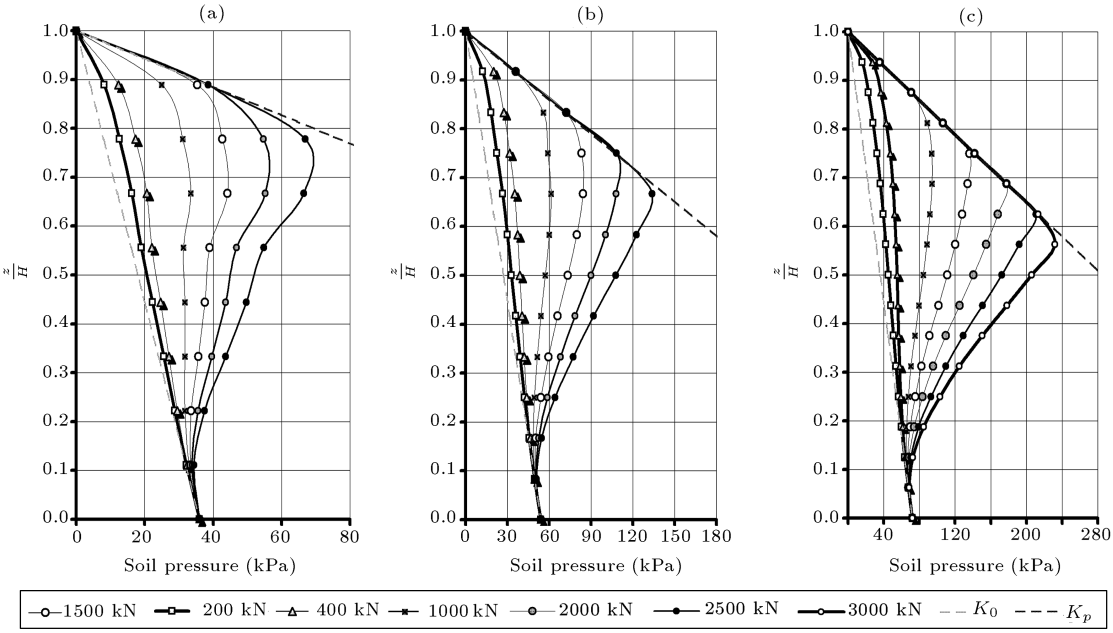

Figure 9. Force-induced soil pressure. (a) 4 m bridge abutment; (b) 6 m bridge abutment; (c) 8 m bridge abutment.

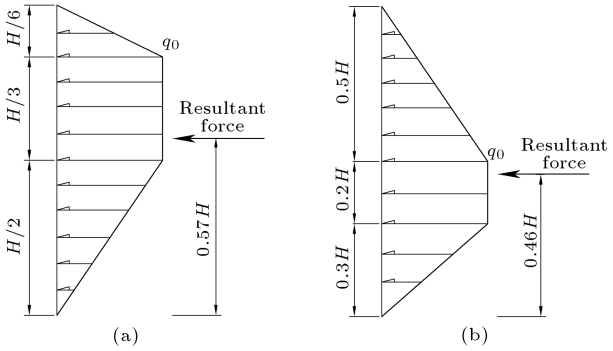

Figure 10. Suggested approximate seismic soil pressure distributions. (a) Type I; (b) Type II.

$$q_0 = \alpha.k_h.\gamma.H, \tag{11}$$

$$q_0 = \beta_1.A_0.\gamma.H, \tag{12}$$

$$q_0 = \beta_2.S.\gamma.H, \tag{13}$$

where:

q_0 = maximum seismic soil pressure.
k_h = seismic horizontal acceleration coefficient.
A_0 = the area under the PSA spectrum between $0.2T$ and $1.5T$ in which T is the period of the first mode of vibration (the spectrum must be in units of m/s^2).
S = Spectral acceleration in units of m/s^2 obtained from the PSA spectrum of an earthquake at the period of vibration for the first mode of the soil-wall system.

α, β_1 and β_2 are coefficients from Tables 1 to 3,

Table 1. Coefficient α and distribution type in α method.

Case	Distribution	α
Bridge abutment ($H < 5$ m)	I	0.31
Bridge abutment ($H \geq 5$ m)	I	0.55
Rigid and propped wall ($H < 5$ m)	I	0.32
Rigid and propped wall ($H \geq 5$ m)	I	0.64
RC retaining wall ($H < 5$ m)	I	0.25
RC retaining wall ($H \geq 5$ m)	II	0.44

Table 2. Coefficient β_1 and distribution type in β_1 method.

Case	Distribution	$\beta 1$
Bridge abutment, rigid wall, and propped wall (independent of height) & RC retaining wall ($H < 5$ m)	I	0.13
RC retaining wall ($H \geq 5$ m)	II	0.07

Table 3. Coefficient β_2 and distribution type in β_2 method.

Case	Distribution	$\beta 2$
Bridge abutment ($H < 5$ m)	I	0.018
Bridge abutment ($H \geq 5$ m)	I	0.03
Rigid and propped Wall ($H < 5$ m)	I	0.019
Rigid and propped Wall ($H \geq 5$ m)	I	0.035
RC retaining wall ($H < 5$ m)	I	0.015
RC retaining wall ($H \geq 5$ m)	II	0.020

adjusting the pressure for wall height and boundary condition.

Distribution type (I or II) shown in Figure 10 is also defined in Tables 1 to 3 for each case with different wall heights and boundary conditions.

Seismic soil pressure distributions introduced above are based on the results of analyses on fixed based models for two reasons. Firstly, to simplify distributions and their corresponding relationships, so that they are independent of soil stiffness, foundation stiffness and foundation width which could complicate the relationships and make them undesirable for design. Secondly, to arrive at a conservative estimate for pressure distributions suitable for design purposes. A fixed-based wall absorbs much more seismic soil pressure than a wall with finite base rotational stiffness. It should be noted that the base rotational fixity is not unreal. For example, the case of pile foundations (usually used in bridge abutments) is very close to base rotational fixity.

Many earthquake records with different intensities and frequency contents and different soil types may be used along with the proposed method suggested in this paper. However, this is deemed unnecessary because the suggested method shows good accordance with other reliable studies in most cases.

The q_0 obtained from Equation 11, which is called the α method herein, is less accurate in comparison with the other two relationships (Equations 12 and 13). This is because the PGA is the simplest and most available parameter of an earthquake and ignores the other characteristics of ground motion. Equations 12 and 13, herein called the $\beta 1$ and the $\beta 2$ methods, give more accurate results but require the PSA spectrum of the input ground motion. In using the β methods, one needs the period of the first mode of vibration (T) for a soil-wall system. Based on the results of modal analyses of several soil-wall systems, the authors suggest Equation 14 or Figure 11 to rapidly obtain T without analysis:

$$T = 0.0029H^2 - 0.0062H + 0.142, \tag{14}$$

where H is the wall height and is restricted between 3 to 10 meters.

Note that for design purposes, the design response spectrum and the PGA of any local seismic design codes can be used as input in α and β methods, respectively.

Total seismic soil thrust against a retaining wall (P_{ST}) for proposed distributions can be obtained as:

Distribution I:

$$P_{ST} = \frac{2}{3} q_0 H. \tag{15}$$

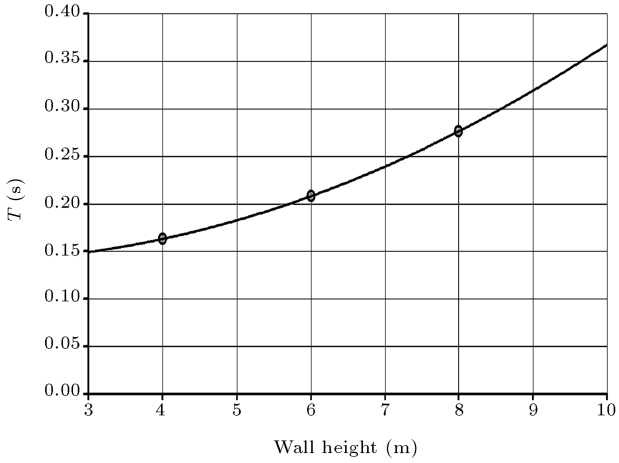

Figure 11. Period of the first mode of vibration (T) for soil-wall systems.

Distribution II:

$$P_{ST} = \frac{3}{5} q_0 H. \tag{16}$$

Figure 12 shows the seismic soil pressures against a 6 m high wall subjected to the San Fernando earthquake, resulted from analyses in different cases. Suggested distributions for seismic soil pressure using the α and β methods are also shown for comparison. As can be seen in Figure 12, the seismic soil pressure is best predicted by the $\beta 1$ method. The α method, although showing more dispersion, gives acceptable results for design purposes. It can also be observed that the suggested distributions are in good agreement with the distributions of seismic soil pressure results from time history analyses of different cases under different earthquakes.

The seismic soil pressures introduced above should be added to the active or at rest soil pressures to acquire the total soil pressure. For rigid and semi-rigid walls (such as bridge abutment and propped bridge abutment), at rest soil pressure is more appropriate, whereas for flexible walls, such as cantilever retaining walls higher than 5 m, active soil pressure should be added to suggested distributions. Figure 13 shows typical total soil pressure distributions for the two cases discussed.

For the case of concentrated lateral force at the top of the abutment (Figure 14a), which usually occurs in bridges during earthquakes, a new distribution for soil pressure is herein introduced and is illustrated in Figure 14b. This distribution has only one parameter, z_0, which is the passive depth defined above. The distribution in depths less than z_0 follows the passive soil pressure and at depths more than 0.9 H follows the at rest soil pressure. Between depths z_0 and $0.9H$, soil pressure linearly decreases from passive to at rest soil pressure. The depth ratio, z_0, can be obtained as

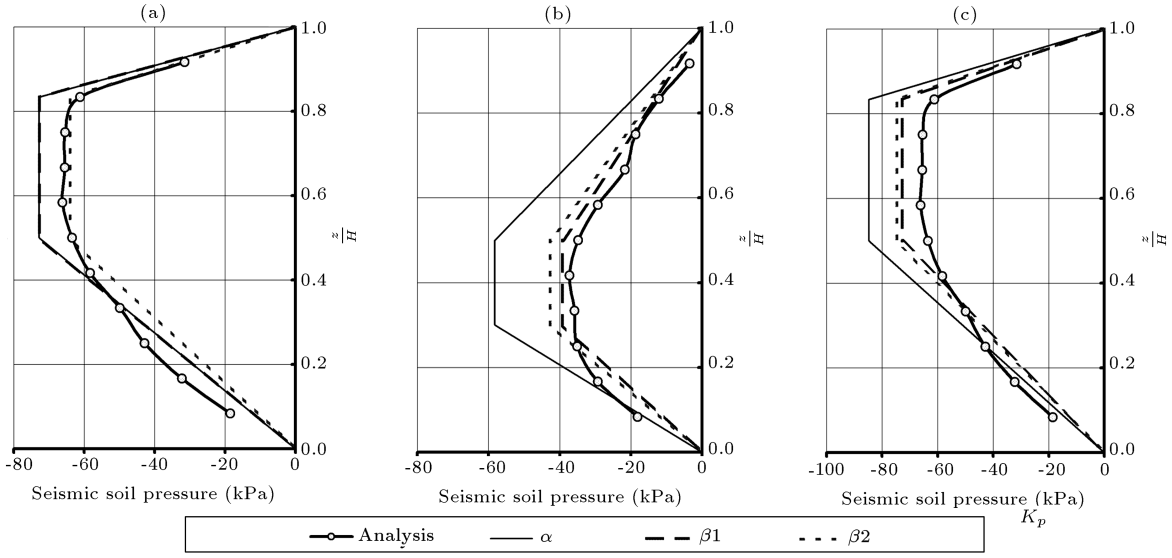

Figure 12. Comparison of seismic soil pressures against a 6 m high wall subjected to San Fernando earthquake, resulted from analysis versus computed values using the proposed α and β methods. (a) Bridge abutment; (b) flexible wall; (c) rigid wall.

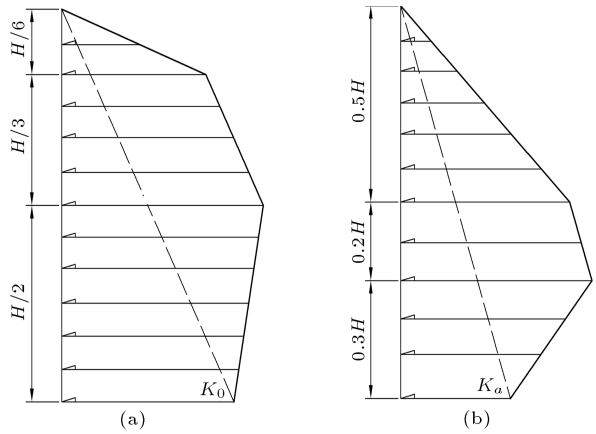

Figure 13. Total soil pressure distribution during earthquake. (a) Type I (rigid or semi-rigid wall); (b) Type II (flexible wall).

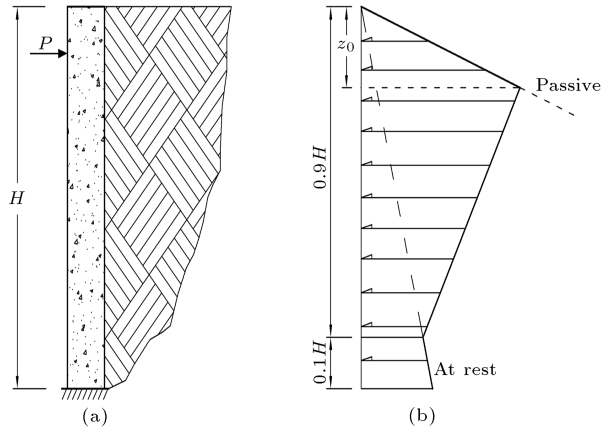

Figure 14. Concentrated lateral force at the top of the abutment. (a) Boundary conditions; (b) suggested soil pressure distribution.

follows:

$$z_0 = \frac{0.004H^{1.6}P^{0.9}}{\gamma(K_p - K_0)}, \tag{17}$$

where:

P	=	external concentrated force at the abutment top along the assumed superstructure's center of mass (for 1 m abutment width) in kN.
H	=	height of the abutment in meters.
K_p, K_0	=	passive and at rest soil pressure coefficients, respectively.

γ is in kN/m^3 and z_0 is in meters.

Figure 15 illustrates the seismic soil pressure caused by a 2000 kN concentrated lateral force at the top of a 6 m high abutment wall resulted from analysis and computed by the above equation. As can be seen in Figure 15, the seismic soil pressure can accurately be predicted by the suggested distribution.

FURTHER VERIFICATION OF THE PROPOSED METHOD

In this section, the proposed seismic pressure values and distribution (Equations 11-13) are compared with the past analytical and experimental research data. Seismic soil pressure for a 4.6 m rigid retaining wall subjected to ATC S1 motion (The ATC recommended motion for S1 soil conditions, PGA = 0.3 g) is calculated using the proposed simplified method and compared with values computed by the SASSI computer

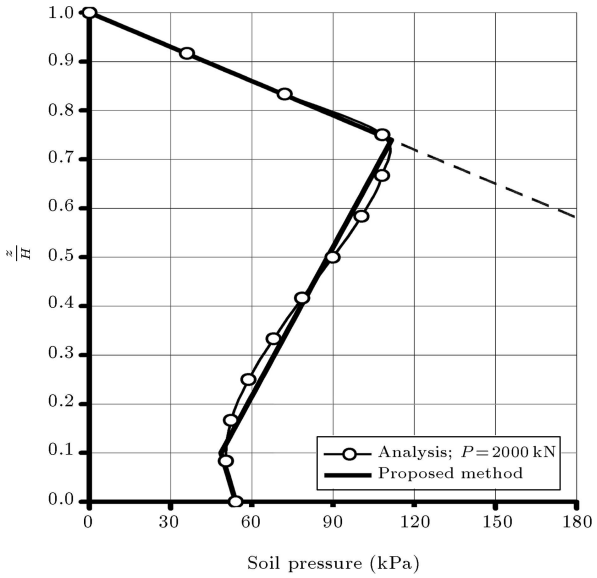

Figure 15. Seismic soil pressure caused by a 2000 kN concentrated lateral force at the top of a 6 m high abutment wall, resulted from analyses and computed by proposed method.

program [24], M-O active earth pressure (using $k_h = 0.3$, $k_v = 0$) and the Ostadan proposed method [27]. The results are shown in Figure 16a. As can be seen in Figure 16a, seismic soil pressure values computed by the proposed method are in good accordance with the two other seismic pressure values and are less than the M-O active earth pressure at depths of more than $0.6H$.

In addition, to verify the proposed seismic soil pressure distribution, normalized seismic soil pressure (soil pressure normalized to 1 at the bottom of the wall for pressure distribution type I) is plotted in Figure 16b against z/H (normalized depth) and compared with the normalized seismic soil pressures presented by the M-O, Wood [6], Ostadan [27], Veletsos and Younan (rigid wall) [12] methods, and also results from the shaking table tests performed by Ohara and Maehara (rigid wall- case compound displacement II) [28] and recently performed centrifuge tests by Nakamura (rigid wall- case 21) [29]. Figure 16b shows that the proposed seismic soil pressure distribution is in good agreement with analytical methods and experimental data presented in the literature.

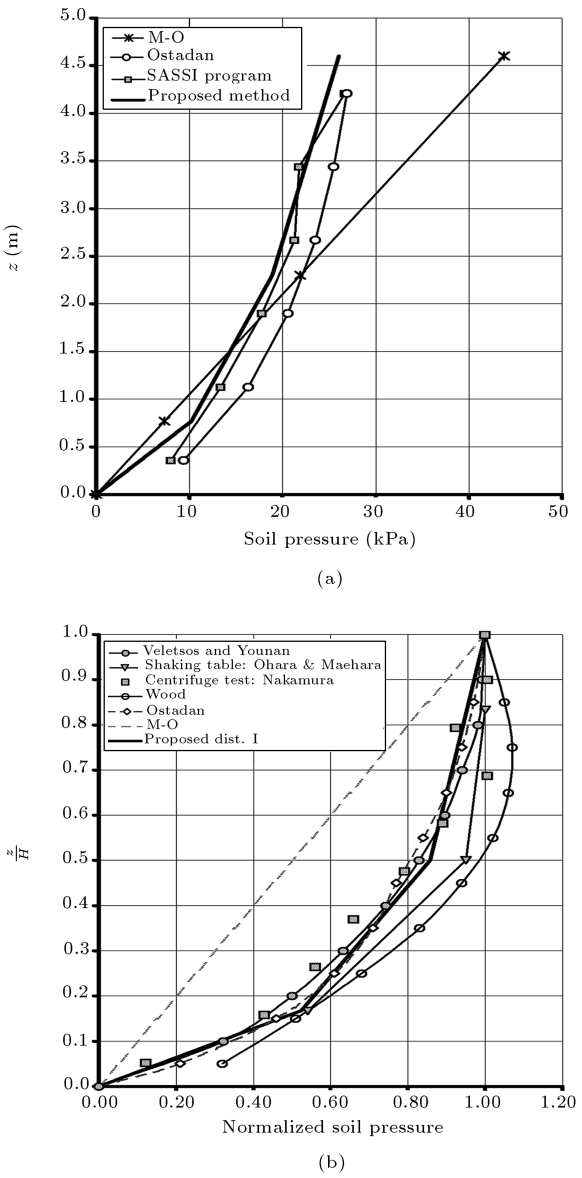

Figure 16. (a) Comparison of proposed seismic soil pressure and computed values with SASSI program and Ostadan method for a 4.6 m wall, $\varphi = 30°$, ATC motion. (b) Comparison of proposed seismic soil pressure distribution with analytical and experimental distributions [6,12,27-29].

SUMMARY AND CONCLUSIONS

In this paper, a method for modeling retaining wall systems was proposed. The model includes free field soil, a retaining wall and springs modeling the interfacing soil. The method is flexible enough to be used under different soil and wall conditions and has satisfactory precision. The popular M-O method's assumptions, such as a rigid gravity wall and a rigid wedge of soil sliding on a linear failure surface, can be criticized, in most cases. This paper's modeling technique is applicable to rigid and flexible walls with different end conditions. Using this model, nonlinear dynamic finite element time history analyses were performed on several soil-wall systems to arrive at the following conclusions:

1. Comparing the results of analyses with the modified M-O [3] method shows that the M-O method is not accurate in every case, but, on average, gives acceptable results for practical purposes.

2. The notion that the seismic soil pressure increases with increasing PGA of an earthquake is not true in every case. It is found that seismic soil pressure is more closely related to the area under the PSA spectrum than the peak ground acceleration of an earthquake.
3. For cantilever walls, seismic soil pressure is greatly influenced by the value of the base rotational stiffness. Maximum soil pressure happens for rigid fixed-base walls.
4. Bridge abutments and propped bridge abutments show similar soil pressure distributions as of rigid walls, but the peak seismic soil pressure is less.
5. Three different methods were proposed for seismic soil pressure distribution against retaining walls (Equations 11-13). These methods are simple to use and show good agreement with nonlinear finite element analyses results, and also past analytical and experimental research data.
6. For the case of a concentrated load applied at the top of an abutment, a simple pressure distribution was also presented (Equation 17).
7. An equation for estimating the first mode period of vibration for the soil-wall system was introduced (Equation 14).

REFERENCES

1. Mononobe, N. and Matsuo, H. "On the determination of earth pressures during earthquakes", *Proc. World Engrg. Conf.*, **9**, paper No. 388, pp. 177-185 (1929).
2. Okabe, S. "General theory of earth pressure", *J. Japanese Soc. of Civ. Engrs.*, **12**(1) (1926).
3. Seed, H.B. and Whitman, R.V. "Design of earth retaining structures for dynamic loads", *The Specialty Conference on Lateral Stresses in the Ground and Design of Earth Retaining Structures, ASCE*, pp. 103-147 (1970).
4. Andersen, G.R., Whitman, R.V. and Geremaine, J.T. "Tilting response of centrifuge-modeled gravity retaining wall to seismic shaking", Report 87-14, Department of Civil Engineering, M.I.T. Cambridge, MA (1987).
5. Sherif, M.A., Ishibashi, I. and Lee, C.D. "Earth pressures against rigid retaining walls", *J. Geotech. Engrg. Div., ASCE*, **108**(5), pp. 679-695 (1982).
6. Wood, J.H. "Earthquake induced soil pressures on structures", Doctoral Dissertation, EERL 73-05, California Institute of Technology, Pasadena, CA (1973).
7. Ishibashi, I. and Fang, Y.S. "Dynamic earth pressures with different wall movement modes, soils and foundations", *Japanese Soc. of Soil Mech. and Found. Engrg.*, **27**(4), pp. 11-22 (1987).
8. Finn, W.D., Yodendrakumar, M., Otsu, H. and Steedman, R.S. "Seismic response of a cantilever retaining wall", *4th Int. Conf. on Soil Dyn. and Earthquake Engrg.*, Southampton, pp. 331-431 (1989).
9. Scott, R.F. "Earthquake-induced pressures on retaining walls", *5th World Conf. on Earthquake Engrg. Int. Assn. of Earthquake Engrg.*, **2**, Tokyo, Japan, pp. 1611-1620 (1973).
10. Veletsos, A.S. and Younan, A.H. "Dynamic modeling and response of soil-wall systems", *J. Geotech. Engrg., ASCE*, **120**(12), pp. 2155-2179 (1994).
11. Richards, R.J., Huang, C. and Fishman, K.L. "Seismic earth pressure on retaining structures", *J. Geotech. Engrg., ASCE*, **125**(9), pp. 771-778 (1999).
12. Veletsos, A.S. and Younan, A.H. "Dynamic response of cantilever retaining walls", *J. Geotech and Geoenviron Engng, ASCE*, **123**, pp. 161-172 (1997).
13. El-Emam, M.M., Bathurst, R.J. and Hatami, K. "Numerical modeling of reinforced soil retaining walls subjected to base acceleration", *Proc. 13th World Conference on Earthquake Engineering*, Vancouver, BC, paper No. 2621 (2004).
14. Green, R.A. and Ebeling, R.M. "Seismic analysis of cantilever retaining walls", Phase I, ERDC/ITL TR-02-3. Information Technology Laboratory, US Army Corps of Engineers, Engineer Research and Development Center, Vicksburg, MS, USA (2002).
15. Puri, V.K., Prakas, S. and Widanarti, R. "Retaining walls under seismic loading", *Fifth International Conference on Case Histories in Geotechnical Engineering*, New York, NY, USA (2004).
16. Green, R.A. and Ebeling, R.M. "Modeling the dynamic response of cantilever earth-retaining walls using FLAC", *3rd International Symposium on FLAC: Numerical Modeling in Geomechanics*, Sudbury, Canada (2003).
17. Cheng, Y.M. "Seismic lateral earth pressure coefficients for $c-\varphi$ soils by slip line method", *Computers and Geotechnics*, **30**(8), pp. 661-670 (2003).
18. Psarropoulos, P.N., Klonaris, G. and Gazetas, G. "Seismic earth pressures on rigid and flexible retaining walls", *Soil Dyn. and Earthquake Engng.*, **25**, pp. 795-809 (2004).
19. Choudhury, D. and Chatterjee, S. "Dynamic active earth pressure on retaining structures", *Sadhana, Academy Proceedings in Engineering Sciences*, **31**(6), pp. 721-730 (2006).
20. Choudhury, D. and Subba Rao, K.S. "Seismic passive resistance in soils for negative wall friction", *Canadian Geotechnical Journal*, **39**(4), pp. 971-981 (2002).
21. Subba Rao, K.S. and Choudhury, D. "Seismic passive earth pressures in soils", *Journal of Geotechnical and Geoenvironmental Engineering, ASCE*, **131**(1), pp. 131-135 (2005).
22. Itasca Consulting Group, Inc. "FLAC (Fast Lagrangian Analysis of Continua) user's manuals", Minneapolis, MN, USA (2000).

23. Schnabel, P.B., Lysmer, J. and Seed, H.B. "SHAKE-A computer program for earthquake response analysis of horizontally layered sites", Earthquake Engineering Research Center, University of California, Berkeley, California, USA (1972).
24. Lysmer, J., Ostadan, F. and Chen, C.C. "SASSI2000-A system for analysis of soil-structure interaction", University of California, Department of Civil Engineering, Berkeley, California, USA (1999).
25. Huang, C. "Plastic analysis for seismic stress and deformation fields", PhD dissertation, Dept. of Civil Engrg., SUNY at Buffalo, Buffalo, NY, USA (1996).
26. Gazetas, G., Psarropoulos, P.N., Anastasopoulos, I. and Gerolymos, N. "Seismic behavior of flexible retaining systems subjected to short-duration moderately strong excitation", *Soil Dyn. and Earthquake Engng.*, **24**, pp. 537-550 (2004).
27. Ostadan, F. "Seismic soil pressure for building walls: An updated approach", *Soil Dynamics and Earthquake Engineering*, **25**, pp. 785-793 (2005).
28. Ohara, S. and Maehara, H. "Experimental studies of active earth pressure", *Memoirs of the Faculty of Engineering*, Yamaguchi University, **20**(1), pp. 51-64 (1969).
29. Nakamura, S. "Reexamination of Mononobe-Okabe theory of gravity retaining walls using centrifuge model tests", *Soils and Foundations*, **46**(2), pp. 135-146 (2006).

BIOGRAPHIES

Shervin Maleki obtained his BS and MS degrees from the University of Texas at Arlington with honors. He then pursued his PhD degree in New Mexico State University at Las Cruces and finished it in 1988. He has many years of experience in structural design, both in the US and Iran. He has been a faculty member at Bradley University in Illinois and Sharif University of Technology in Iran. He has authored and/or coauthored over forty technical papers and has authored two books and a chapter in the Handbook of International Bridge Engineering to be published in 2011. His research area is mainly focused on the Seismic Design of Bridges and Buildings. He has also patented a seismic damper in Iran.

Saeed Mahjoubi started his university studies in 2000 at Sharif University of Technology (SUT) in Iran in the field of Civil Engineering. Having finished his undergraduate studies in 2004, he continued as a graduate student at SUT in Structural Engineering. He successfully defended his thesis entitled "Seismic Behavior of Integral Abutment Bridges" to obtain his MS degree in 2006. He was accepted as a PhD student at SUT in 2008. During his graduate studies he attended several international conferences to present his research which is mainly focused on Bridge Seismic Analysis and Retrofit (Structural Engineering World Congress, Bangalore, 2007; 3rd International Bridge Conference, Tehran, 2008, and 2 articles presented at the 8th International Congress on Civil Engineering, Shiraz, 2009).